Analysis of *S*-rich $CuIn(S,Se)_2$ layers for photovoltaic applications: Influence of the sulfurization temperature on the crystalline properties of electrodeposited and sulfurized $CuInSe_2$ precursors

V. Izquierdo-Roca,[1] A. Pérez-Rodríguez,[1,a] J. R. Morante,[1] J. Álvarez-García,[2] L. Calvo-Barrio,[3] V. Bermudez,[4] P. P. Grand,[4] L. Parissi,[4] C. Broussillon,[4] and O. Kerrec[4]
[1]*EME/CERMAE/IN²UB, Departament d'Electrònica, Universitat de Barcelona, C. Martí i Franquès 1, 08028 Barcelona, Spain*
[2]*Centre de Recerca i Investigació de Catalunya (CRIC), Trav. de Gràcia 108, 08012 Barcelona, Spain*
[3]*Lab. Anàlisis de Superficies, SCT, Universitat de Barcelona, C. Lluis Solé i Sabarís 1-3, 08028 Barcelona, Spain*
[4]*Institute of Research and Development of Photovoltaic Energy (IRDEP) (UMR 7174, CNRS/EDF/ENSCP), 6 Quai Watier, BP 49, 78401 Chatou Cedex, France*

(Received 31 December 2007; accepted 10 April 2008; published online 23 June 2008)

This paper reports the microstructural analysis of *S*-rich $CuIn(S,Se)_2$ layers produced by electrodeposition of $CuInSe_2$ precursors and annealing under sulfurizing conditions as a function of the temperature of sulfurization. The characterization of the layers by Raman scattering, scanning electron microscopy, Auger electron spectroscopy, and XRD techniques has allowed observation of the strong dependence of the crystalline quality of these layers on the sulfurization temperature: Higher sulfurization temperatures lead to films with improved crystallinity, larger average grain size, and lower density of structural defects. However, it also favors the formation of a thicker MoS_2 interphase layer between the $CuInS_2$ absorber layer and the Mo back contact. Decreasing the temperature of sulfurization leads to a significant decrease in the thickness of this intermediate layer and is also accompanied by significant changes in the composition of the interface region between the absorber and the MoS_2 layer, which becomes Cu rich. The characterization of devices fabricated with these absorbers corroborates the significant impact of all these features on device parameters as the open circuit voltage and fill factor that determine the efficiency of the solar cells. © *2008 American Institute of Physics*. [DOI: 10.1063/1.2939833]

I. INTRODUCTION

Thin film solar cell technologies are an attractive alternative in terms of cost to crystalline and multicrystalline silicon cells. Chalcopyrite photovoltaic technology has already reached a mature state, being currently produced at an industrial scale. In particular, by modifying the composition and growth conditions of $Cu(In,Ga)(S,Se)_2$ alloys, it has been possible to optimize the optoelectronic properties of these absorbers, which have been proven to be able to render efficiencies above 19%.[1] In a constant effort toward reducing the manufacturing cost of chalcopyrite photovoltaic modules, an active research is currently ongoing in order to develop new, scalable manufacturing processes based on nonvacuum deposition technologies. In this sense, electrodeposition methods are highly interesting approaches for producing large area modules. In recent years, many fundamental and technological problems related to the electrodeposition of semiconducting materials have been overcome, and efficiencies up to 11% have been achieved using absorbers produced using a two step process.[2] In the first step, $CuInSe_2$ precursor nanocrystalline layers are obtained by means of electrochemical methods. In order to improve the crystalline quality of the films, these precursors are annealed under sulfurizing conditions, resulting in $CuIn(S,Se)_2$ absorbers with good optoelectronic characteristics. However, the efficiencies obtained with electrodeposited films are still below those attained with similar chalcopyrite absorbers grown using conventional vacuum-based processes.

Optimization of the optoelectronic properties of electrodeposited absorbers requires a deeper understanding of the properties of the material, as well as of the influence of the different growth parameters involved in film formation. In previous works, we presented a detailed Raman spectroscopy characterization study of electrodeposited $CuInSe_2$ precursor films, as well as annealed absorbers.[3] The present paper aims to investigate the influence of the annealing temperature on the crystalline properties of the final absorbers. As it will be shown, this parameter has a critical influence on the quality and properties of the layers, which in turn has a significant impact on the characteristics of the solar cells fabricated with these absorbers.

II. EXPERIMENTAL

S-rich $CuIn(S,Se)_2$ absorber layers have been grown on a Mo coated glass using a two step process. First, a nanocrystalline $CuInSe_2$ precursor layer was obtained by electrodeposition in an acidic bath containing Cu_2^+, In_3^+, and H_2SeO_3 electroactive species. Electrodeposition conditions were chosen in order to produce films with overall stoichiometry given by $In/Cu=0.9$ and $Se/(Cu+In)=1.2$. After

[a]Electronic mail: aperezro@el.ub.es.

 © 2008 American Institute of Physics

Downloaded 14 Jun 2010 to 161.116.168.169. Redistribution subject to AIP license or copyright; see http://jap.aip.org/jap/copyright.jsp

electrodeposition, the films were annealed in a sulfur containing atmosphere using a rapid thermal process. In order to investigate the effect of the sulfurization temperature on the film properties, precursor layers have been processed using three different nominal temperatures (T_{nom} of 550, 600, and 680 °C). In the experimental setup, the nominal temperature is controlled by two thermocouple sensors: One is used as a reference for the furnace power control and the second one is placed in the back of the cell (which means just below the glass), giving us the temperature at this point. Due to the thermal resistance of the glass substrates (which are 3 mm thick), measured temperatures overestimate the actual film temperature during the annealing process. At the temperature range of interest, the absolute error in the temperature was found to be between +30 and +50 °C, according to the reference measurements carried out in equivalent heating processes with the measure thermocouple just on the surface of a virgin glass substrate. According to these measurements, the actual sulfurization temperatures were in the range between 520 and 630 °C. After the sulfurization reaction, the absorbers were treated in a NaCN bath in order to etch the Cu-rich excess segregating at the surface of the films in the form of Cu(S,Se) phases. Selected samples from these absorbers were used for the fabrication of solar cell devices. In this case two further process steps were applied to the samples, corresponding to the chemical bath deposition of a thin CdS buffer layer and the rf sputtering of the ZnO window layer.

Samples obtained were characterized by means of Raman spectroscopy combined with optical microscopy, scanning electron microscopy (SEM), x-ray diffraction (XRD), and Auger electron spectroscopy (AES). Raman microprobe measurements were performed using a T64000 Jobin-Yvon spectrometer coupled to an Olympus metallographic microscope. Excitation was provided with the 514.5 nm emission line of an Ar^+ laser. Measurements were made in a backscattering configuration using a 100× (NA=0.95) microscope objective, providing a submicronic spot size. Laser power was limited to 0.5 mW in order to avoid thermal effects on the spectra. Under these conditions, the estimated irradiance on the samples was about 150 kW/cm^2.

A Hitachi S-4100 scanning electron microscope was used in order to investigate the nanostructure and morphology of the layers. In-depth chemical compositional profiles were obtained by means of AES using a Phi 670 scanning Auger nanoprobe. The electron gun parameters selected for the measurements were electron beam energy of 10 keV and filament current of 10 nA. The scanned area for the AES measurements was about 10×10 μm^2 for a focused beam diameter below 100 nm. For the in-depth measurements, ion sputtering was carried out with an Ar^+ beam with energy below 5 keV in order to avoid inducing significant damage.

Combined in-depth Raman/AES measurements were also performed by acquiring sequentially a series of Raman spectra after sputtering the sample in the AES system between every Raman measurement. Since the penetration depth of the green light in $CuIn(Se,S)_2$ is only around 100 nm, this procedure allows obtaining complete information of the bulk of the films. A detailed description of this combined technique can be found elsewhere.[4]

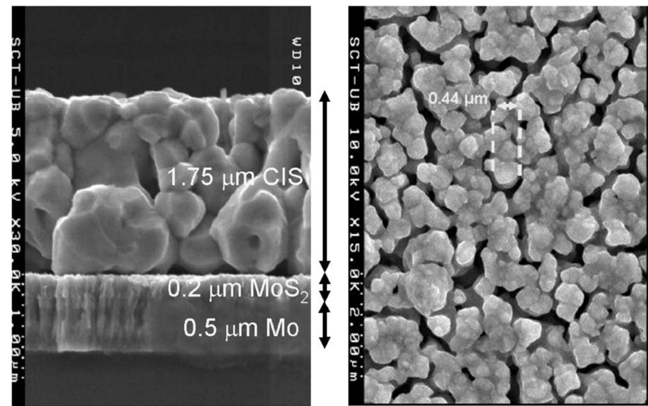

FIG. 1. SEM cross section (left) and top view (right) images obtained from the precursor annealed at the lowest temperature (T_{nom}=550 °C).

$2\theta/\theta$ XRD measurements were carried out in a Phillips MRS diffractometer, and Ω-scan XRD measurements were done in a Siemens D-500 diffractometer using the $K\alpha$ emission line of copper. Finally, the microstructural analysis of the layers was correlated with the parameters of the final devices. The efficiency of the solar cells was derived from $I(V)$ measurements performed at room temperature using a solar simulator at standard air mass 1.5 conditions.

III. MICROSTRUCTURAL ANALYSIS: EXPERIMENTAL RESULTS

A. Morphological characterization

Figure 1 shows SEM pictures obtained from samples grown at the lowest temperature (T_{nom}=550 °C). In the cross section image the molybdenum coated glass substrates, onto which the absorber layers are formed, can be appreciated. In this case, the $CuIn(S,Se)_2$ phase exhibits a polycrystalline microstructure with a quite large dispersion in the grain size, which varies roughly from 100 nm to 1 μm. Even though the film appears compact, it is still possible to appreciate the presence of some voids. The poor compactness of the sample is more evident in the top view SEM image of this sample, where it can also be observed that the grains tend to group, forming cluster structures. This microstructure is a direct result of the annealing process, which on the one hand promotes the sulfurization and growth of the nanometric precursor crystallites, and on the other hand favors the coalescence of the grains. However, it can be observed that in the case of the sample processed at 550 °C, the thermal energy provided by the annealing process is not able to completely recrystallize the clusters, which finally results in the presented microstructure. Furthermore, the cross section image also reveals the presence of an intermediate layer between the Mo and the $CuIn(S,Se)_2$ ones. The estimated thickness of this layer is about 200 nm and presents a characteristic and distinctive columnar structure. This layer has been found to be constituted primarily by MoS_2, as will be shown in the next sections.

Downloaded 14 Jun 2010 to 161.116.168.169. Redistribution subject to AIP license or copyright; see http://jap.aip.org/jap/copyright.jsp

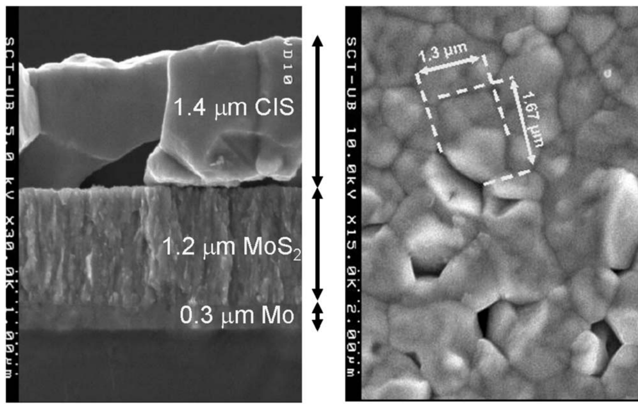

FIG. 2. SEM cross section (left) and top view (right) images obtained from the precursor annealed at the highest temperature (T_{nom}=680 °C).

The effect of increasing the annealing temperature on the film morphology can be observed in Fig. 2. The most noticeable effect is the increase in the average grain size (above 1 μm) and film compactness. Moreover, a second important effect is the increase in the thickness of the MoS_2 intermediate layer which, according to the cross section images, attains a total thickness of the order of 1.2 μm.

B. Raman/AES measurements

Raman spectra were obtained from the surface of samples annealed at three different temperatures (see Fig. 3). In principle, the main peaks in the Raman spectra from $CuIn(S,Se)_2$ correspond to the A_1 symmetry zone-center phonon band of the chalcopyrite structure that shows a bimodal behavior with two bands involving pure S–S and Se–Se vibrations.[5] The spectra measured in the samples are characterized by a dominant peak, which corresponds to the S–S vibrational mode. The position of this band is close to the reference position obtained from a $CuInS_2$ single crystal (290 cm^{-1}). This indicates that during the annealing process sulfur replaces most of the selenium atoms originally present in the precursor nanocrystals. Nevertheless, the different sulfurization temperature is responsible for notorious differences in the spectra: As shown in Fig. 3, decreasing the temperature of sulfurization leads to a blueshift and an asymmetric broadening of the peak, with an increase in the contribution at higher wavenumbers. As will be discussed in the next sections, these effects have been attributed to an increase in the density of crystalline defects in the samples annealed at lower temperatures.

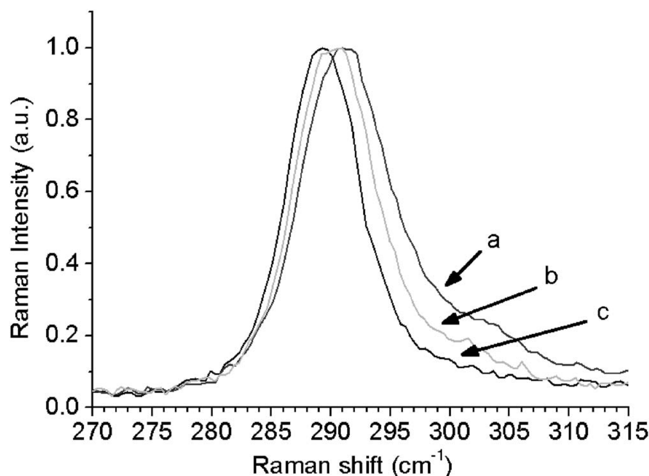

FIG. 3. Raman spectra obtained from the surface of the three samples annealed at different nominal temperatures: (a) 550 °C, (b) 600 °C, and (c) 680 °C.

Due to the exceptionally high absorption coefficient of $CuInS_2$, the information provided by surface Raman analysis is restricted by the penetrating light in the material to the first 100 nm of the film. Nevertheless, the chemical and crystalline properties of the bulk of the films can be assessed by using ion sputtering to etch the surface of the film. This procedure has been systematically carried out by combining Raman and AES measurements, as described in the experimental section. Figure 4 shows the Raman spectra and AES compositional depth profile for a sample grown at T_{nom} =550 °C. AES profiles show a bulk stoichiometry close to $CuInS_2$, with a slightly Cu depleted region only on the film surface. Such deviation appears to be characteristic of $CuIn(S,Se)_2$ compounds and has been associated in the literature with an accumulation of a high number of vacancies leading to the presence of ordered vacancy compound secondary phases on the surface region of the layers.[6,7] Furthermore, Raman spectra from the bulk of the sample confirm that the film is constituted by chalcopyrite ordered $CuInS_2$, even though the crystalline quality of this phase worsens toward the back interface, as can be appreciated by a significant broadening of the A_1 band. The Raman spectra measured in this region also show a broad contribution in the 320–360 cm^{-1} spectral range. This could be related to the presence in the layers of $CuIn_5S_8$ domains.[8] Approaching the Mo back region, two bands clearly emerge in the spectra at 378 and 403 cm^{-1}. These bands prove the formation of a MoS_2 intermediate layer during the sulfurization process.[9] The existence of this phase is also noticeable in the AES profiles, which show a sulfur enrichment in the region where the Mo signal starts to grow. In addition, AES profiles also reveal the accumulation of Cu immediately above the MoS_2 intermediate region.

The samples grown at T_{nom}=680 °C present a similar bulk compositional profile with a slight In-rich composition, as shown in Fig. 5. Deconvolution of the bulk Raman spectra reveals that the width of the A_1 chalcopyrite band is smaller in the case of the sample grown at the highest temperature, which indicates that the crystalline quality of the chalcopyrite phase is improved by higher annealing temperatures. The spectra measured in this region also show a broad contribution at the 320–360 cm^{-1} region that could be indicative of the presence of the $CuIn_5S_8$ spinnel secondary phase. On the other hand, it is worth noting the increase in the thickness of the MoS_2 intermediate layer between the absorber and the Mo ones, which is evidenced in the AES profile. In this case, this intermediate layer shows a significant content (in the range of 5%–10%) of Cu. This is also accompanied by a significant decrease in the Cu content in the region of the absorber close to the interface of the MoS_2 layer. The Raman spectra from this layer are characterized by the presence of the bands' characteristic of pure MoS_2 appearing close to

Downloaded 14 Jun 2010 to 161.116.168.169. Redistribution subject to AIP license or copyright; see http://jap.aip.org/jap/copyright.jsp

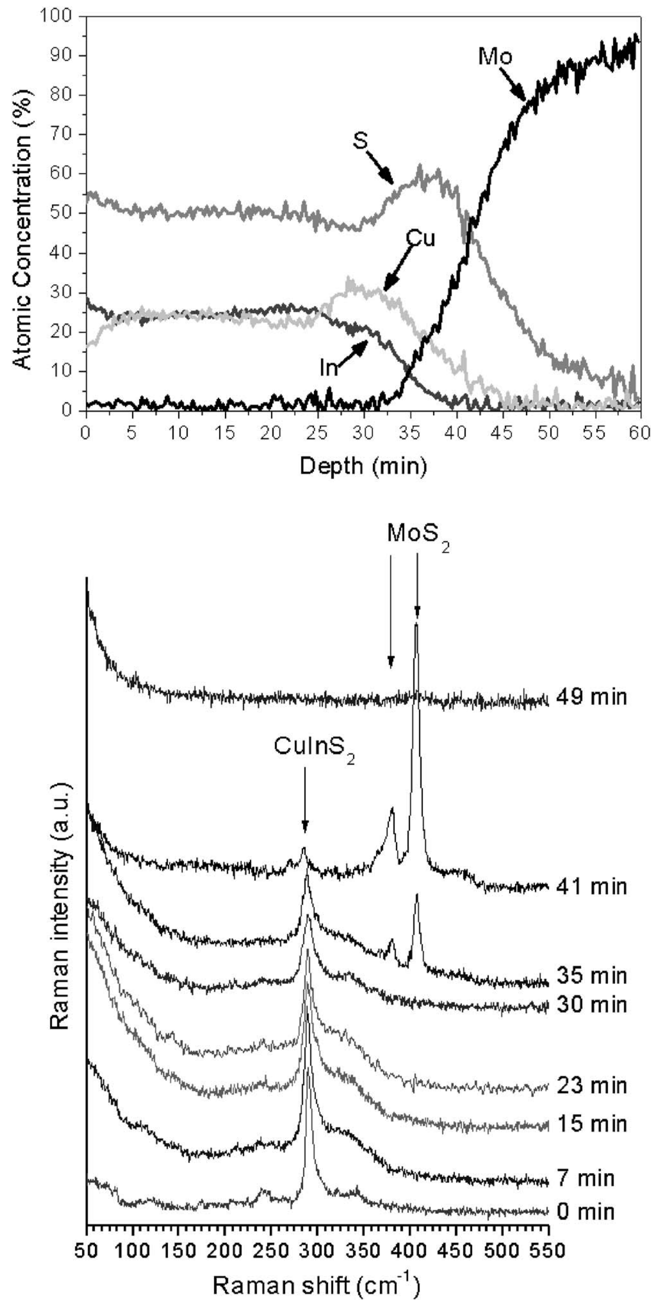

FIG. 4. AES depth profile (top) and Raman spectra measured at different depths (bottom) from the sample annealed at $T_{nom}=550$ °C.

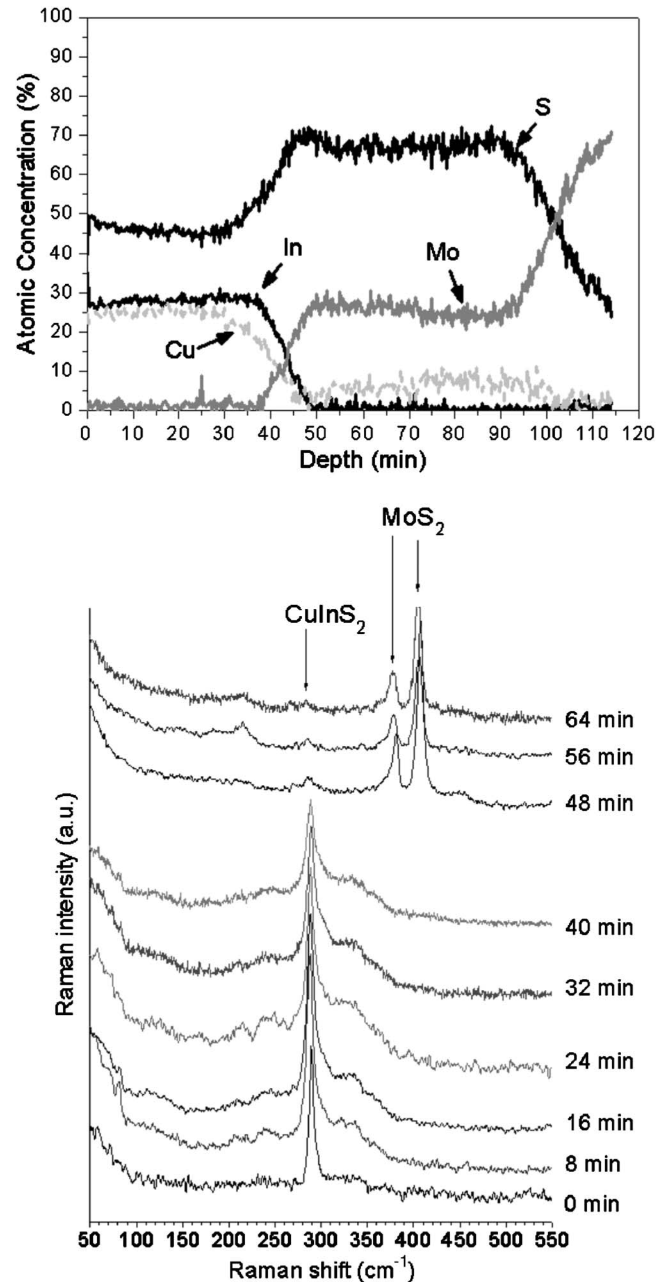

FIG. 5. AES depth profile (top) and Raman spectra measured at different depths (bottom) from the sample annealed at $T_{nom}=680$ °C.

their reference position. Accordingly, no indications of Cu alloying within the MoS_2 are observed in the spectra. Furthermore, some low intensity bands arise in the spectra close to the interface region (145, 185, and 213 cm^{-1}), which may be directly related to the presence of Cu observed in the AES profiles (see Fig. 6). These bands are tentatively attributed to a Cu-rich phase, though we have not been able to assign them to any referenced compound in the literature. The identification of the origin of these modes requires a further analysis of these layers.

C. X-ray diffraction measurements

Figure 7 shows the $2\theta/\theta$ diffractograms obtained from the samples grown at highest and lowest temperatures (680 and 550 °C, respectively). The diffractograms clearly indicate the presence of the cubic Mo phase, with a quite clear texture in the (110) direction. In addition, they also contain reflections characteristic of the chalcopyrite structure of the $CuInS_2$ compound, with a slightly preferential texture in the (112) direction. An interesting difference between the two diffractograms deals with the presence of additional reflections at 32.8°, 58.3°, 68.7°, and 96.7°. Initially, these reflections were attributed to the presence in the layers of $CuIn_5S_8$ and $CuIn_5S_9$ phases. This was done from the analysis of the samples grown at the highest temperature, taking into account the slightly In-rich composition of the absorbers and the evidence in the in-depth Raman spectra, suggesting the presence of $CuIn_5S_8$.[3] However, the analysis of a broader ensemble of samples has allowed the observation of a direct

Downloaded 14 Jun 2010 to 161.116.168.169. Redistribution subject to AIP license or copyright; see http://jap.aip.org/jap/copyright.jsp

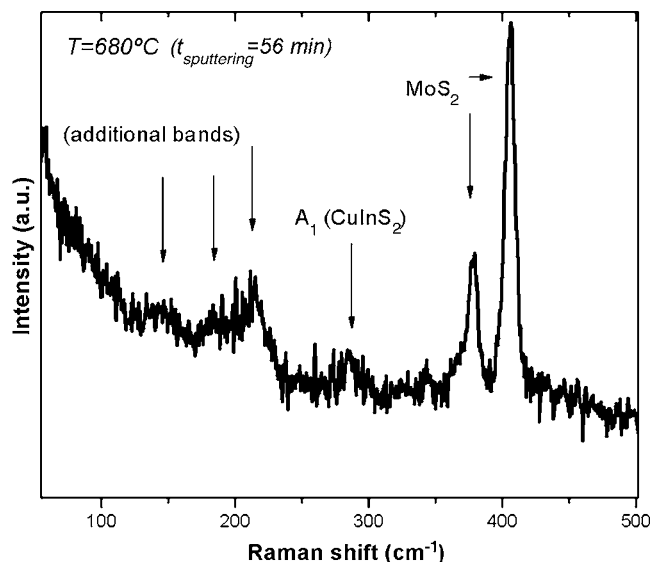

FIG. 6. Raman spectrum obtained from the bulk of samples annealed at T_{nom}=680 °C after a sputtering time of 54 min, showing the presence of additional bands that may be related to a Cu-rich phase.

correlation of the intensity of these reflections with the thickness of the intermediate MoS_2 layer. This leads to the assignment of these relatively broad bands to the (101), (110), (021), and (211) reflections of MoS_2. The relative intensity of these peaks in the diffractograms suggests the presence of the rhombohedral ($R3m$) MoS_2 phase. However, taking into account the strong similarities between the XRD diffractograms from both rhombohedral and hexagonal phases of MoS_2, the presence of the hexagonal MoS_2 phase in the samples cannot be excluded. The assignment of these bands to this compound is also supported by ω-scan measurements, which show that their intensity increases close to the intermediate region between the absorber and the back Mo contact. Moreover, the absence of a (003) reflection points out that MoS_2 grows preferentially with the *c axis* of the crystallographic structure parallel to the surface.

IV. DISCUSSION

The changes observed in the main A_1 $CuInS_2$ mode in the Raman spectra from the samples sulfurized at different temperatures are related to the presence of crystalline defects in the absorbers: Lower annealing temperatures produce films with higher density of crystalline defects, which lead to shorter phonon lifetimes in the crystals. As a result, the bandwidth of the A_1 band is substantially larger in the case of the samples obtained at lower temperatures. Furthermore, the lower crystalline quality of samples processed at lower temperatures has two additional effects on the spectra. First, it induces a clear asymmetry in the A_1 band. Second, it leads to a gradual (blue) shift of the A_1 band toward higher wavenumbers. XRD stress measurements reveal the presence of stress levels in the chalcopyrite phase from the different samples close to the uncertainty of the measurements, with

FIG. 7. XRD diffractograms from samples annealed at T_{nom}=680 °C and T_{nom}=550 °C.

Downloaded 14 Jun 2010 to 161.116.168.169. Redistribution subject to AIP license or copyright; see http://jap.aip.org/jap/copyright.jsp

compressive stress values in the 10–50 MPa range. These stress values are too low to explain the observed shift of the Raman band. Furthermore, both effects (blueshift and asymmetric broadening of the A_1 peak) are interpreted as direct results of the higher density of crystalline defects present in samples annealed at lower temperatures. The presence of defects relaxes the momentum conservation rule in the crystal, thus making possible the participation of noncenter phonons in the Raman process. As a result, the line shape of the Raman peak is ultimately determined by the number of defects, the density of states of phonons, and the shape of phonon dispersion curves. This is supported by a theoretical calculation of the A_1 $CuInS_2$ dispersion curves, which show a positive slope in the vicinity of the Γ point of the Brillouin zone.[10,11] Then, the blueshift and band asymmetry toward high wavenumbers are basically a consequence of this positive slope of the dispersion curves of the A_1 band close to the center of the Brillouin zone.

The presence of a higher density of defects in the samples sulfurized at lower temperatures is also accompanied by a significant decrease in the open circuit voltage (V_{oc}) in the solar cells, from values of 0.75 V (sample sulfurized at $T_{nom}=680$ °C) down to 0.66 V (sample sulfurized at $T_{nom}=550$ °C). This is related to the dependence of V_{oc} on the density of defects acting as recombination centers in the space charge region of the devices,[11,12] which are also contributing to the activation of noncenter phonons in the Raman spectra. This, together with the worsening of the layer crystallinity, contributes to the observed decrease in the efficiency of the devices: Cells fabricated with absorbers synthesized at the highest temperature of 680 °C have typical efficiency values of $\eta \sim 8.5\%$, and this parameter decreases down to $\eta \sim 6\%$ when the temperature of sulfurization decreases down to 550 °C.

On the other hand, increasing the sulfurization temperature also favors the growth of a thicker intermediate MoS_2 layer between the absorber layer and the back Mo contact. In principle, the presence of this phase is desirable in terms of avoiding the formation of a rectifying union in the back contact. Evidence on the presence of a very thin interfacial MoS_2 layer region have also been reported for $CuInS_2$ absorbers synthesized using conventional vacuum based processes,[9,13] this being similar to the thin interfacial $MoSe_2$ layer observed at the back region from $Cu(In,Ga)Se_2$ absorbers.[7] In relation to these works, the electrodeposited samples are characterized by the presence of a thicker MoS_2 interfacial layer. This is specially true for the samples sulfurized at the highest temperature, where the thickness of the intermediate MoS_2 layer becomes comparable to that of the absorber. This could be favored by the preferential growth of this layer with the *c* axis of the crystallographic structure parallel to the surface, according to the XRD data. In this sense, the higher diffusivity of Cu in crystalline directions perpendicular to the (003) one would allow the synthesis of thicker MoS_2 layers, this behavior being enhanced at higher sulfurization temperatures. The presence of a thick MoS_2 layer could contribute to an increase in the serial resistance of the solar cell device, thus degrading its performance.

However, in spite of this behavior, the analysis of the $I(V)$ characteristics of the devices measured under illumination shows similar values of the serial resistance of cells fabricated with absorbers sulfurized at different temperatures, which is kept at around 4.5 Ω cm^2. This suggests that the increase in the thickness of the MoS_2 layer does not contribute to the increase in the serial resistance of the device. Then, the decrease in the efficiency of the devices sulfurized at lower temperatures is mainly related to the decrease in V_{oc} and the fill factor, which would be determined by the presence of a higher density of structural defects in the absorbers, as suggested by the Raman spectra. This also correlates with the existence of significant changes in the composition of the interface region between the absorber and the MoS_2 one, which can also contribute to the observed variations in the parameters of the solar cell devices. Lower sulfurization temperatures lead to an interface region with a high Cu content, as shown in the in-depth AES composition profiles. This correlates with the existence of a Cu excess in the interface region between the $CuInSe_2$ electrodeposited absorbers and the back Mo layer.[14] After annealing, it is not clear whether this Cu excess is accommodated inside the chalcopyrite structure, or it indeed corresponds to a segregation of a binary Cu_xS_y compound. The absence of covellite (CuS) characteristic bands in the Raman spectra excludes the presence of this phase, which is known to yield intense bands at 19 and 475 cm^{-1}.[15] However, the complexity of the Cu–S phase diagram makes it difficult to exclude the presence of other phases with lower Raman signals, such as Cu_3S_2, $Cu_{2-x}S$, and CuS_2. Increasing the temperature of sulfurization favors diffusion of Cu into the thicker MoS_2 layer, which likely determines the formation of a Cu depleted interface region. This could also be favored by a higher surface segregation of excess Cu in the form of Cu-rich secondary phases.[3] This implies the need to improve the knowledge of the structural composition of the film close to the back contact in order to precisely model the performance of solar cell devices based on these absorbers.

V. CONCLUSIONS

In this paper we have investigated the effect of the annealing temperature on the crystalline properties of $CuInS_2$ films obtained from the sulfurization of electrodeposited $CuInSe_2$ nanocrystalline precursors and their impact on the solar cell characteristics. Higher sulfurization temperatures lead to films with improved crystallinity and larger average grain size. However, it also favors the formation of a thicker MoS_2 interphase layer between the $CuInS_2$ absorber layer and the Mo back contact, as supported from the SEM, Raman, AES, and XRD measurements. The analysis of the $I(V)$ characteristics of the solar cells shows a decrease in the efficiency of the devices fabricated with the absorbers sulfurized at lower temperatures. This is related to the worsening of the layer crystallinity and the increase in the density of structural defects (as deduced from the Raman spectra) observed when the temperature of sulfurization decreases. On the other hand, the degradation of the solar cell parameters also correlates with an accumulation of Cu close to the MoS_2 interface, as revealed by the AES profiles. The presence of

Downloaded 14 Jun 2010 to 161.116.168.169. Redistribution subject to AIP license or copyright; see http://jap.aip.org/jap/copyright.jsp

this Cu excess may be responsible for the apparition of unidentified additional bands in the Raman spectra from the bulk of the samples. This suggests the need to improve the degree of control of the structure and composition of the interface region between the absorber and the back MoS_2 layer, in addition to the crystalline quality of the absorber, for the optimization of the efficiency of the devices.

ACKNOWLEDGMENTS

EME is a member of CEMIC (Centre of Microsystems Engineering) of the Generalitat de Catalunya. This work was funded by the LARCIS project (Grant No. SES6-CT-2005-019757) of the Sixth FM Programme of the European Commission.

[1]M. A. Contreras, K. Ramanathan, J. AbuShama, F. Hasoon, D. L. Young, B. Egaas, and R. Noufi, Prog. Photovoltaics **13**, 209 (2005).
[2]D. Lincot, J. F. Guillemoles, S. Taunier, D. Guimar, J. Sicx-Kurdi, A. Chaumont, O. Roussel, O. Ramdani, C. Hubert, J. P. Fauvarque, N. Bodereau, L. Parissi, P. Panheleux, P. Fanouillere, N. Naghavi, P. P. Grand, M. Benfarah, P. Mogensen, and O. Kerrec, Sol. Energy **77**, 725 (2004).
[3]V. Izquierdo-Roca, A. Pérez-Rodríguez, A. Romano-Rodríguez, J. R. Morante, J. Álvarez-García, L. Calvo-Barrio, V. Bermudez, P. P. Grand, O. Ramdani, L. Parissi, and O. Kerrec, J. Appl. Phys. **101**, 103517 (2007).
[4]L. Calvo-Barrio, A. Pérez-Rodríguez, J. Álvarez-García, A. Romano-Rodríguez, B. Barcones, J. R. Morante, K. Siemer, I. Luck, R. Klenk, and R. Scheer, Vacuum **63**, 315 (2001).
[5]R. Bacewicz, W. Gebicki, and J. Filipowicz, J. Phys.: Condens. Matter **6**, L777 (1994).
[6]K. Müller, R. Sheer, Y. Burkov, and D. Schmeißer, Thin Solid Films **451–452**, 120 (2004).
[7]H. W. Schock and U. Rau, Physica B (Amsterdam) **308–310**, 1081 (2001).
[8]N. M. Gasanly, S. A. El-Hamid, L. G. Casanova, and A. Z. Magomedov, Phys. Status Solidi B **169**, K115 (1992).
[9]J. Álvarez-García, A. Pérez-Rodríguez, A. Romano-Rodríguez, J. R. Morante, L. Calvo-Barrio, R. Scheer, and R. Klenk, J. Vac. Sci. Technol. A **19**, 232 (2001).
[10]J. Lazewski, P. T. Jochym, and K. Parlinski, J. Chem. Phys. **117**, 2726 (2002).
[11]E. Rudigier, Ph.D. thesis, Philipps-Universität Marburg, 2004.
[12]V. Izquierdo, A. Pérez-Rodríguez, L. Calvo-Barrio, J. Álvarez-García, J. R. Morante, V. Bermúdez, O. Ramdani, J. Kurdi, P. P. Grand, L. Parissi, and O. Kerrec, Thin Solid Films, "Raman scattering microcrystalline assessment and device quality control of electrodeposited CuIn(S,Se)2 based solar cells" (unpublished).
[13]R. Scheer and H.-J. Lewerenz, J. Vac. Sci. Technol. A **13**, 1924 (1995).
[14]O. Ramdani, Ph.D. thesis, Université Pierre et Marie Curie (Paris 6), 2007.
[15]M. Ishii, K. Shibata, and H. Nozaki, J. Solid State Chem. **105**, 504 (1993).

Downloaded 14 Jun 2010 to 161.116.168.169. Redistribution subject to AIP license or copyright; see http://jap.aip.org/jap/copyright.jsp